Coupled Microwave Billiards as a Model for Symmetry Breaking

H. Alt,[1] C. I. Barbosa,[2] H.-D. Gräf,[1] T. Guhr,[2] H. L. Harney,[2] R. Hofferbert,[1] H. Rehfeld,[1] and A. Richter[1]
[1]*Institut für Kernphysik, Technische Universität Darmstadt, D-64289 Darmstadt, Germany*
[2]*Max-Planck-Institut für Kernphysik, D-69029 Heidelberg, Germany*
(Received 6 July 1998)

Two superconducting microwave billiards have been electromagnetically coupled in a variable way. The spectrum of the entire system has been measured and the spectral statistics analyzed as a function of the coupling strength. It is shown that the results can be understood in terms of a random matrix model of quantum mechanical symmetry breaking—as, e.g., the violation of parity or isospin in nuclear physics. [S0031-9007(98)07757-6]

PACS numbers: 05.45.+b, 11.30.Er, 24.60.Lz

Both classical and quantum mechanical chaos can be studied with the help of billiards; see, e.g., the recent review [1]. Quantum mechanical billiards are readily simulated by sufficiently flat microwave resonators [2–5] since the Schrödinger and the Helmholtz equations are equivalent in two dimensions. Here, we present a study of a system consisting of two coupled resonators. This simulates the breaking of a symmetry; see below. The resonators were made superconducting. This allowed us to study the transition from the uncoupled case into the regime of weak coupling very precisely. The positions of the resonances were determined with a precision of 10^{-7}.

Symmetry breaking in chaotic systems has been intensely investigated. Impressive is the study of parity violation in heavy nuclei [6]. Atomic and molecular symmetries were studied in [7,8]. Another example from nuclear physics is isospin mixing; see, e.g., [9,10]. In [10], the complete spectrum of the nucleus ^{26}Al at low excitation energy was established. The analysis of this spectrum in terms of the so-called Gaussian orthogonal ensemble (GOE) of random matrices showed that the level statistics was intermediate between a 2-GOE and a 1-GOE behavior [11]. By this, we refer to the following model. Each level in the spectrum of ^{26}Al can be characterized by isospin 0 or 1. In the absence of mixing, the spectrum of the states of each isospin (i.e., of each symmetry class) has the statistical properties of the eigenvalues of matrices belonging to the GOE. The superposition of the two spectra displays a 2-GOE behavior. It is described by the first term of the Hamiltonian

$$\mathcal{H} = \begin{pmatrix} \boxed{\text{GOE}} & 0 \\ 0 & \boxed{\text{GOE}} \end{pmatrix} + \alpha \begin{pmatrix} \boxed{0} & V \\ V^{+} & \boxed{0} \end{pmatrix}. \quad (1)$$

This is a special case of the model of Ref. [7]. The off-diagonal matrix couples the classes. The random elements in the GOEs and in V, all have the same rms value v so that $\alpha = 1$ makes $\mathcal{H}$ as a whole to be a GOE matrix. The resulting spectrum displays 1-GOE behavior. For the observables studied below, the 1-GOE behavior is actually reached already if $\alpha v/D$ is ≈ 1. Here, D is the mean level distance of $\mathcal{H}$. For simplicity, we set $v = 1$ in the sequel. This makes D dimensionless and the parameter governing the level statistics is then α/D. In the example of ^{26}Al, this parameter was determined from the level statistics; whence the mean square Coulomb matrix element that breaks isospin was derived. The present experiment tests the model (1) with a large number of levels and very clean spectra in a situation, where the parameter α/D controlling the symmetry breaking can be varied. Alternative models for coupled chaotic systems are, e.g., given in [12,13].

In the present experiment each of the two symmetry classes consists of the eigenstates of a (quarter of a) stadium billiard; see Fig. 1. The radius of the quarter circle was in both cases $r = 0.2$ m. The ratios γ between the length of the rectangular part and r were $\gamma_1 = 1$ and $\gamma_2 = 1.8$ for the two billiards, respectively. The measurement was restricted to frequencies below 16 GHz where both resonators are two dimensional and display 608 and 883 resonances, respectively. For the variable superconducting coupling, the two resonators were put on top of each other and holes, 4 mm in diameter, were drilled through the 2 mm thick walls of both resonators (see Fig. 2). A niobium washer ensured sufficient electrical contact between the resonators. Coupling was achieved through a niobium pin, 2 mm in diameter, which could be moved perpendicularly to the plane of the billiards from outside the helium cryostat by a drive. The coupling strength is determined by the depths x_1 and x_2 by which the niobium pin penetrates into the γ_1 and γ_2 stadium, respectively. For the strongest coupling, a second niobium pin, penetrating all the way through both resonators, was added. Stronger coupling could have been obtained by using even more coupling pins. This was,

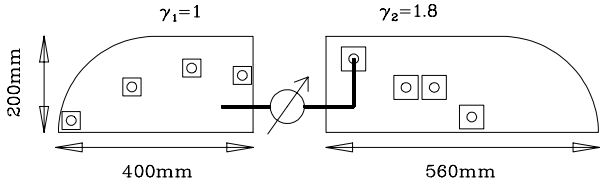

FIG. 1. Shapes and locations of the antennas of the two coupled Bunimovich stadium billiards.

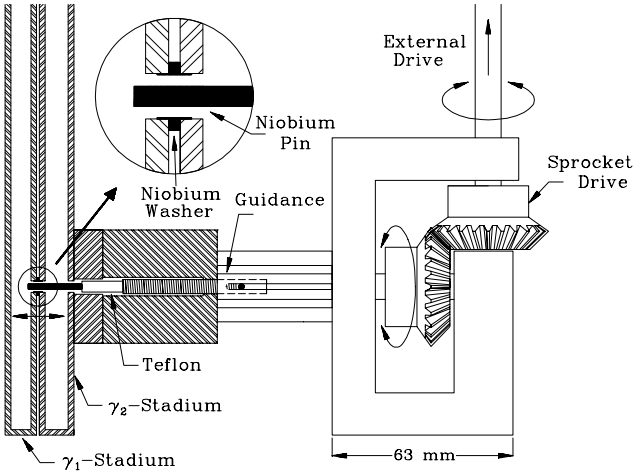

FIG. 2. The adjustable superconducting coupling.

however, not realized since it was the particular emphasis of the present experiment to study the transition from the uncoupled case into the weakly coupled regime.

For each of the couplings we have measured the complete spectrum in steps of 10 kHz. In doing so, half of the microwave power was fed into each of the resonators. The states of the γ_1 stadium were not always visible through an antenna connected to the γ_2 stadium, and vice versa. Therefore the spectrum of the entire system was constructed by adding the spectra obtained through the seven antennas, four on the γ_1 stadium and three on the γ_2 stadium; see Fig. 1.

A small frequency range of spectra at various couplings is shown in Fig. 3. One recognizes that the resonances are shifted by statistically varying amounts. The observed frequency shifts result from the coupling of the two cavities and from the perturbation of the electromagnetic field by the pin. The latter effect was investigated separately by inserting (or not) the pin into the γ_2 stadium only. Under that condition when only the field is perturbed but no coupling is achieved all measured spectra (see, e.g., top of Fig. 4) displayed a clean 2-GOE behavior. The mean level spacing is $D = 10.7$ MHz. The resonance widths are of the order of 1 to 100 kHz. The high Q of 10^5–10^6 together with the very good signal-to-noise ratio of up to 50 dB of the superconducting setup was obviously necessary to detect the partly small shifts, and thus the dependence of the level statistics on the coupling.

We now turn to the analysis of the spectra. From the ansatz (1), the nearest-neighbor spacing distribution (NND), the Σ^2 statistic and the Δ_3 statistic can be obtained numerically; see [11,14] and results below. Although the coupling parameter α/D can be determined by comparing numerical simulations with the data, it is convenient to have analytical expressions of Σ^2, etc., as functions of α/D. French *et al.* [14] and Leitner *et al.* [15] have derived them for small coupling parameters using perturbation theory.

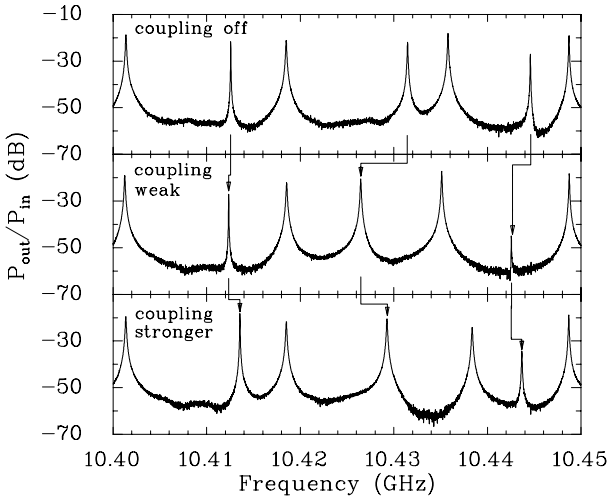

FIG. 3. A small frequency range of three spectra with different coupling. The arrows are intended to help to recognize the shifts of a few resonances.

The analysis of the present data has been based on the Σ^2 statistic or number variance

$$z(L) = \langle [n(L) - L]^2 \rangle . \tag{2}$$

Here, $n(L)$ is the number of eigenvalues in an interval of length L. To obtain $z(L)$, we divided the entire unfolded spectrum of length ND into $N_L = N/L$ adjacent intervals of length L and took the average $\langle\,\rangle$ over these. By looking at the correlation between $z(L)$ and $z(L + \varepsilon)$, we convinced ourselves that $z(L)$ and $z(L + \varepsilon)$ were statistically independent for $\epsilon \geq 0.025$—at least in the range

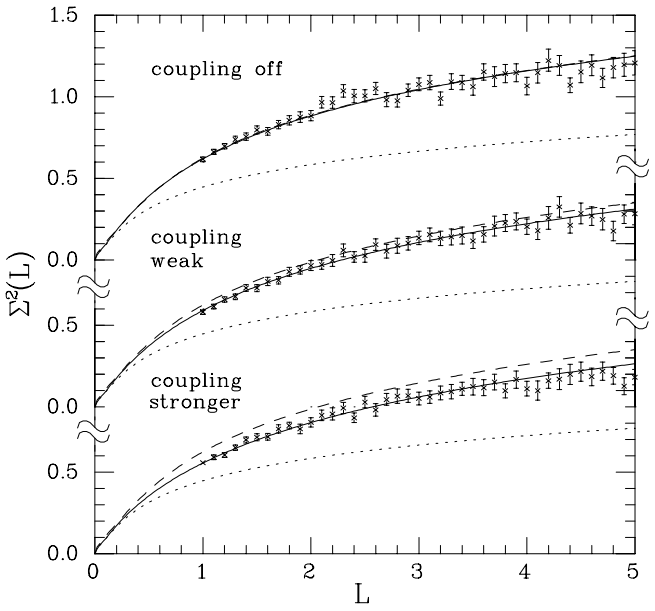

FIG. 4. The Σ^2 statistic for three different couplings. The dotted line gives the 1-GOE and the dashed line the 2-GOE behavior. The solid lines result from the estimation of α/D described in the text and correspond to the first, the third, and the last entry of Table I.

$1 \le L \le 5$. Calculating $z(L)$ in that range in steps of $\varepsilon = 0.025$ has provided $M = 161$ experimental numbers $z(L_k)$, $k = 1 \ldots M$, that were statistically independent as is needed for the fit procedure described below. The upper limit $L \le 5$ is defined by the saturation of the Σ^2 statistic [16]: Random matrix theory is known to describe spectral fluctuations of chaotic systems up to a maximum $L_{\max}$ which is related to the length of the shortest periodic orbit. This sets $L \le 5$ here. To check the influence of the saturation, we restricted the extraction of α/D to $L \le 3$. The slight change of the results was well within the errors. The lower limit of $1 \le L$ is explained in the sequel.

The expectation value $\overline{z(L)}$ is called $\Sigma^2(L, \Lambda)$, where $\Lambda = (\alpha/D)^2$. According to Ref. [15], this function is

$$\Sigma^2(L, \Lambda) = \Sigma^2(L, \infty) + \frac{1}{\pi^2} \ln\left(1 + \frac{\pi^2 L^2}{4(\tau + \pi^2 \Lambda)^2}\right). \tag{3}$$

Here, $\Sigma^2(L, \infty)$ is the limiting function for the 1-GOE system. The parameter τ is related to the ratio of dimensions in the GOE blocks of Eq. (1). One finds $\tau = 0.74$ in the present case.

In order to estimate α/D, one has to know the probability distribution $w_k[z(L_k) \,|\, \Lambda]$, $k = 1 \ldots M$, of every data point. By applying the "bootstrap method" [17] to the set of N_{L_k} intervals from which $z(L_k)$ was calculated, we found w_k to be a χ^2 distribution with average value as given by (3) and with roughly N_{L_k} degrees of freedom—which is reasonable. However, this was true only for $L_k \ge 1$. For $L_k < 1$, no analytical representation of the distribution of $z(L_k)$ was found. At the same time, the information on Λ is lost: for small L, the relative change of Σ^2 with Λ is of the order of L while the relative rms deviation of z is of the order of $L^{1/2}$. Therefore, the analysis was restricted to $L_k \ge 1$.

The joint distribution $W(z \,|\, \Lambda) = \prod_k w_k[z(L_k) \,|\, \Lambda]$ of all the $z(L_k)$ was converted into the distribution $W(\Lambda \,|\, z)$ of Λ with the help of Bayes' theorem

$$W(\Lambda \,|\, z) = \frac{W(z \,|\, \Lambda)\mu(\Lambda)}{\int d\Lambda W(z \,|\, \Lambda)\mu(\Lambda)}. \tag{4}$$

The *a priori* distribution of Λ was defined as

$$\mu(\Lambda) = \left| \int d^M z W(z \,|\, \Lambda) \frac{\partial^2}{\partial \Lambda^2} \ln W(z \,|\, \Lambda) \right|^{1/2} \tag{5}$$

since this expression ensures that—at least for sufficiently large M—the entropy

$$H = -\int d^M z W(z \,|\, \Lambda) \ln\left(\frac{W(z \,|\, \Lambda)}{\int d\Lambda W(z \,|\, \Lambda)\mu(\Lambda)}\right) \tag{6}$$

of $W(z \,|\, \Lambda)$ is independent of Λ, whence Λ cannot be estimated by a maximum entropy argument without any experiment.

The center and the rms deviation of the distribution (4) were determined if it was Gaussian. This defines the best estimate and the error of Λ as well as α given in Table I. For three cases (part of) the data and the fit function (3) that results from the best estimate are given in Fig. 4. In the case of zero coupling, $P(\Lambda \,|\, z)$ was not a Gaussian and the result given in Table I is an upper limit for the confidence of 68%.

A χ^2 test—generalized to the case of non-Gaussian distributions w_k—has shown that for the fits reported in Table I, the analytical model (3) of [15] is compatible with the data. To check that the perturbation result (3) does apply to our case, we also performed numerical simulations of the full model (1) using the procedure described in [11]. Thereby we obtained values for α/D which cannot be affected by limitations of the perturbative calculation of [15]. However, reassuringly, the results of both analyses are consistent within the errors.

From the coupling parameter and the mean level spacing $D = 10.7$ MHz, one obtains the rms coupling matrix element α of the model (1). It corresponds to the rms Coulomb matrix element $\sqrt{\langle H_C^2 \rangle}$ that is responsible for isospin mixing [11]. Figure 4 shows that starting from 2-GOE behavior in the uncoupled case ($\alpha/D \le 0.024$) one moves through the weakly coupled case ($\alpha/D = 0.13$) towards 1-GOE behavior. The strongest coupling ($\alpha/D = 0.20$) realized here causes, however, still a relatively weak symmetry breaking of about the same size as the isospin symmetry breaking in ^{26}Al. The spreading width $\Gamma^{\downarrow}/D = 2\pi(\alpha/D)^2$ which is a measure of how much the states of the two symmetry classes are mixed into each other, is also given in Table I. In the case of the strongest coupling, e.g., one sees that a state of class 1 carries about 25% admixture of class 2 and vice versa. This is the reason for the shifts observed in Fig. 3.

The fact that the level statistics depend on α proves that the coupling block V in the Hamiltonian (1) is essentially filled with statistically independent elements—as we have assumed. If—on the contrary—V were a separable interaction coupling only one specific configuration of the first symmetry class to one in the second class, then the level statistics would not change as a function of α.

We finally note that there is an experiment similar to the present one performed with elastomechanical resonances in quartz blocks [18]. Both experiments in

TABLE I. Mixing parameters for six different coupling strengths resulting from the Bayesian analysis described in the text. The penetration depths of the coupling pin into the resonators is given by (x_1, x_2) in mm. The results of the bottom row were obtained using a second coupling pin.

Physical coupling	α/D	α (MHz)	$\Gamma^{\downarrow}/D$
(0,8)	≤ 0.029	≤ 0.31	≤ 0.0054
(5,3)	0.105 ± 0.008	1.12 ± 0.08	0.07 ± 0.01
(4,4)	0.130 ± 0.007	1.39 ± 0.07	0.11 ± 0.01
(5,8)	0.173 ± 0.006	1.85 ± 0.06	0.19 ± 0.01
(6,8)	0.180 ± 0.006	1.93 ± 0.06	0.20 ± 0.01
(6,8)	0.200 ± 0.006	2.14 ± 0.06	0.25 ± 0.01

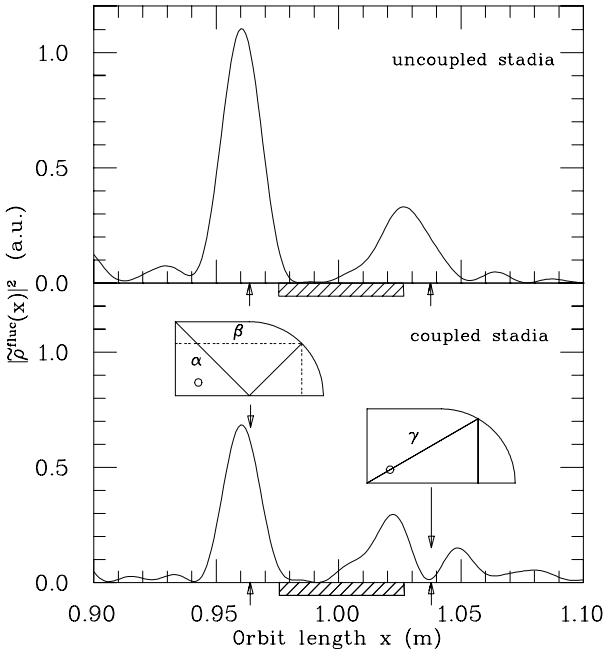

FIG. 5. Fourier transforms of the spectra of the uncoupled and a coupled system. The lengths of the periodic orbits α, β, γ (shown in the insets) are indicated by the arrows. The lengths of the whispering gallery orbits are located within the hatched area. Orbit γ touches the coupling pin which is marked by circles in the insets.

principle allow semiclassical interpretations. The periodic orbits for [18] are, however, very complicated. For the present relatively simple system, we have tried to detect periodic orbits that run back and forth through both of the coupled billiards. Systematic variations of the integrated level density—including those caused by the bouncing ball orbits—have been removed as described in [5]. The Fourier transform $\tilde{\varrho}^{\,\mathrm{fluc}}(x)$ of the remaining fluctuating part is expected to display the lengths x of the periodic classical orbits of the system [19]. In $\tilde{\varrho}^{\,\mathrm{fluc}}(x)$ obtained from the coupled stadia we have not been able to identify a peak introduced by the coupling and corresponding to an orbit running through both stadia. A very small part of the results is given in Fig. 5. In the range of x which is displayed, there are periodic orbits only in the γ_1 stadium. The shortest orbit of the γ_2 stadium is at 1.19 m. Introduction of the coupling changes $\tilde{\varrho}^{\,\mathrm{fluc}}(x)$ at every x—whether or not the orbits of length $\approx x$ came close to the coupling pin. This is expected because $|\tilde{\varrho}^{\,\mathrm{fluc}}(x)|^2$ obeys a sum rule: The total intensity $\int dx|\tilde{\varrho}^{\,\mathrm{fluc}}(x)|^2$ is given by the number of states. It is, however, interesting to see that a rather drastic change occurs in the vicinity of orbit γ. The peak at $x \approx 1.03$ m (uncoupled case) splits into two (coupled case) and the interference minimum occurs at γ, i.e., the orbit γ touches the coupling pin.

In summary, the dependence of the spectral statistics on the coupling between levels belonging to different symmetry classes has been demonstrated for a system that simulates quantum chaos. Even subtle changes of the level statistics induced by small coupling parameters could be observed. The present experiment models mixing between any two symmetry classes.

We would like to thank O. Bohigas, G. E. Mitchell, H.-J. Stöckmann, and H. A. Weidenmüller for very helpful discussions. This work has been supported by the Sonderforschungsbereich 185 "Nichtlineare Dynamik" of the Deutsche Forschungsgemeinschaft. One of us (C. I. B.) acknowledges support by the Fritz Thyssen Stiftung.

[1] T. Guhr, A. Müller-Groeling, and H. A. Weidenmüller, Phys. Rep. **299**, 189 (1998).
[2] H.-J. Stöckmann and J. Stein, Phys. Rev. Lett. **64**, 2215 (1990).
[3] E. Doron, U. Smilansky, and A. Frenkel, Phys. Rev. Lett. **65**, 3072 (1990).
[4] S. Sridhar, Phys. Rev. Lett. **67**, 785 (1991).
[5] H.-D. Gräf *et al.*, Phys. Rev. Lett. **69**, 1296 (1992).
[6] J. D. Bowman *et al.*, Annu. Rev. Nucl. Part. Sci. **43**, 829 (1993).
[7] N. Rosenzweig and C. E. Porter, Phys. Rev. **120**, 1698 (1960).
[8] E. Haller, H. Köppel, and L. S. Cederbaum, Chem. Phys. Lett. **101**, 215 (1983).
[9] H. L. Harney, A. Richter, and H. A. Weidenmüller, Rev. Mod. Phys. **58**, 607 (1986).
[10] G. E. Mitchell *et al.*, Phys. Rev. Lett. **61**, 1473 (1988).
[11] T. Guhr and H. A. Weidenmüller, Ann. Phys. (N.Y.) **199**, 412 (1990).
[12] O. Bohigas, S. Tomsovic, and D. Ullmo, Phys. Rev. Lett. **65**, 5 (1990).
[13] T. Dittrich, H. Schanz, and G. Koboldt (to be published).
[14] J. B. French *et al.*, Ann. Phys. (N.Y.) **181**, 198 (1988).
[15] D. M. Leitner, Phys. Rev. E **48**, 2536 (1993); D. M. Leitner, H. Köppel, and L. S. Cederbaum, Phys. Rev. Lett. **73**, 2970 (1994).
[16] M. V. Berry, Proc. R. Soc. London A **400**, 229 (1985).
[17] B. Efron and R. J. Tibshirani, *An Introduction to the Bootstrap* (Chapman and Hall, New York, 1993).
[18] C. Ellegaard *et al.*, Phys. Rev. Lett. **77**, 4918 (1996).
[19] M. C. Gutzwiller, *Chaos in Classical and Quantum Mechanics* (Springer, New York, 1980).